C10(EO)4-8SH paper

DATASET · OCTOBER 2012

READS
18

7 AUTHORS, INCLUDING:

David J Vanderah
Institute for Bioscience and Biotechnology R…
90 PUBLICATIONS **1,860** CITATIONS
SEE PROFILE

Thomas B Parr
University of Delaware
38 PUBLICATIONS **46** CITATIONS
SEE PROFILE

Curtis W Meuse
National Institute of Standards and Technolo…
64 PUBLICATIONS **1,310** CITATIONS
SEE PROFILE

Gintaras Valincius
Vilnius University
82 PUBLICATIONS **1,089** CITATIONS
SEE PROFILE

Characterization of a Series of Self-Assembled Monolayers of Alkylated 1-Thiaoligo(ethylene oxides)$_{4-8}$ on Gold

David J. Vanderah,*,†,1 Congtam P. Pham,† Stephanie K. Springer,† Vitalii Silin,‡ and Curtis W. Meuse*,†,1

Biotechnology Division, Chemical Science and Technology Laboratory, National Institute of Standards and Technology, Gaithersburg, Maryland 20899-8313, and Georgetown University, Washington, D.C. 20057

Received December 29, 1999. In Final Form: May 16, 2000

Self-assembled monolayers of a series of linear thiols containing a 1-thiaoligo(ethylene oxide) (TOEO) moiety, i.e., $HS(EO)_xR$ (where $R = C_{10}H_{21}$, $EO = -CH_2CH_2O-$, and $x = 4-8$), were prepared on polycrystalline gold and characterized by visible spectroscopic ellipsometry (SE), infrared spectroscopic ellipsometry, and surface plasmon resonance. The TOEO segment was found to adopt a 7/2 helical structure oriented normal to the substrate for $x = 5-7$. Different structures were found for the other compounds in this series. When $x = 4$, the TOEO segment adopts a predominantly trans-extended conformation, whereas when $x = 8$, the TOEO appears to be disordered with some helical conformation. Monolayer thicknesses determined by SE are consistent with these structural changes. The significant increase in disorder with extension of the hydrophilic segment by two ethylene oxide units from 6 to 8 is potentially valuable for protein reconstitution in supported hybrid bilayer constructs.

Introduction

Interest in transmembrane and integral-membrane proteins for sensor and biomedical applications continues to increase.[2,3] Future technologies based on membrane proteins will require supporting matrixes approximating or "mimicking" natural bilayers.[4] Natural bilayer components provide a "fluid" environment, have polar groups that match polar protein regions, and impose only small spatial restrictions on both sides of the membrane. These properties allow membrane proteins to easily incorporate, adopt native conformations, deploy extramembranous segments, and undergo conformational changes, if necessary, during interactions with other biomolecules. Various strategies to construct effective supporting matrixes at or near a surface have been reported.[5−10] Hybrid bilayer membranes (HBMs) consisting of an inner layer of *n*-alkanethiol self-assembled monolayers (SAMs) on Au and an outer layer of phospholipid were found to be rugged and to exhibit insulating properties similar to those of natural bilayers.[11,12] However, protein incorporation into HBMs with *n*-alkanethiol SAM inner layers will not be optimal because alkanethiol layers are highly ordered, adopt structures that maximize interactions between neighboring chains, and do not provide the proper polar environment for water and extramembranous protein segments. These properties would render protein incorporation more difficult and could adversely affect protein structure and function, as was observed in recent experiments with the pore-forming toxin α-hemolysin in a HBM ($C_{18}H_{37}SH$/egg−phosphatidylcholine).[13]

SAMs of thiols that contain hydrophilic functional groups or segments that provide a hydrophilic spacer proximal to the substrate surface would most likely be less ordered than unfunctionalized alkanethiols and would more closely resemble the amphiphilic nature of natural bilayer components.[4,14] As part of an ongoing effort to identify amphiphiles for HBM constructs, we recently reported the synthesis of new thiols of the general structure $HS(EO)_6R$, where $R = C_nH_{2n+1}$ or C_nD_{2n+1} (n = 10 or 18) and $EO = CH_2CH_2O$ [**1**−**4**; see Table 1], and characterized their SAMs on Au.[15] Surprisingly, we found that the SAMs of **1**−**4** were highly ordered in *both* the alkyl and the 1-thiahexa(ethylene oxide) (THEO) segments. Analysis of the C−H stretching region of the reflection absorption infrared spectroscopy (RAIRS) spectra indicated that the alkyl segments of the SAMs of **1**−**4** were in a nearly all-trans conformation, similar to that of the corresponding *n*-alkanethiol SAMs.[16] The order of the alkyl segments was found to increase with an increase in the length of the hydrocarbon chain and, for **3**, a tilt angle of 32° ± 2° from the substrate normal and a twist angle of −30° ± 2° were determined.[15] In addition, electrochemical blocking experiments using potassium ferricyanide indicated packing densities for the SAMs of

* To whom correspondence should be directed.
† National Institute of Standards and Technology.
‡ Georgetown University.
(1) E-mail: djvander@mailserver.nist.gov; curtis.meuse@nist.gov.

(2) Plant, A. L. *Langmuir* **1999**, *15*, 5128 and references therein.
(3) Kasianowicz, J. J.; Brandin, E.; Branton, D.; Deamer, D. W. *Proc. Natl. Acad. Sci.* **1996**, *93*, 13770.
(4) Duschl, C.; Liley, M.; Lang, H.; Ghandi, A.; Zakeeruddin, S. M.; Stahlberg, H.; Dubochet, J.; Nemetz, A.; Knoll, W.; Vogel, H. *Mater. Sci. Eng.* **1996**, *C4*, 7.
(5) Toby, A.; Jebkins, A.; Boden, N.; Bushby, R. J.; Evans, S. D.; Knowles, P. F.; Miles, R. E.; Ogier, S. D.; Schönherr, H.; Vancso, G. J. *J. Am. Chem. Soc.* **1999**, *121*, 5274.
(6) Yang, Z.; Yu, H. *Langmuir* **1999**, *15*, 1731.
(7) Raguse, B.; Braach-Maksvytis, V.; Cornell, B. A.; King, L. G.; Osman, P. D. J.; Pace, R. J.; Wieczorek, L. *Langmuir* **1998**, *14*, 648.
(8) Sachmann, E. *Science* **1996**, *271*, 43 and references therein.
(9) Plant, A. L.; Gueguetchkeri, M.; Yap, W. *Biophys. J.* **1994**, *67*, 1126.
(10) Duschl, C.; Liley, M.; Corradin, G.; Vogel, H. *Biophys. J.* **1994**, *67*, 1229.
(11) Meuse, C. W.; Niaura, G.; Lewis, M. L.; Plant, A. L. *Langmuir* **1998**, *14*, 1604.
(12) Plant, A. L. *Langmuir* **1993**, *9*, 2764.
(13) Glazier, S. A.; Vanderah, D. J.; Plant, A. L.; Bayley, H.; Valincius, G.; Kasianowicz, J. J. *Langmuir*, in press.
(14) Lang, H.; Duschl, C.; Vogel, H. *Langmuir* **1994**, *10*, 197.
(15) Vanderah, D. J.; Meuse, C. W.; Silin, V.; Plant, A. L. *Langmuir* **1998**, *14*, 6916.
(16) Nuzzo, R. G.; Fusco, F. A.; Allara, D. L. *J. Am. Chem. Soc.* **1987**, *109*, 2358.

10.1021/la9916833 CCC: $19.00
Published on Web 07/18/2000

Table 1. Structures and Monolayer Thickness Data of 1-Thia-ω-Alkylated Oligo(ethylene oxide)$_x$ Amphiphiles, Where x = 4−8, and Related Compounds

	structure	*d* (nm) ellipsometry[a]	*d* (nm) SPR[b]
1	$HS(CH_2CH_2O)_6C_{10}H_{21}$	3.1[c]	3.0
2	$HS(CH_2CH_2O)_6C_{10}D_{21}$	3.1[c]	
3	$HS(CH_2CH_2O)_6C_{18}H_{37}$	4.1[c]	5.0[d]
4	$HS(CH_2CH_2O)_6C_{18}D_{37}$	4.2[c]	
5	$HS(CH_2)_{11}(OCH_2CH_2)_6OH$	2.7[e]	
6	$HS(CH_2)_{15}CONH(CH_2CH_2O)_6H$	3.9[f]	
7	$HS(CH_2CH_2O)_4C_{10}H_{21}$	3.4	3.4
8	$HS(CH_2CH_2O)_5C_{10}H_{21}$	3.0	2.8
9	$HS(CH_2CH_2O)_7C_{10}H_{21}$	3.3	2.7
10	$HS(CH_2CH_2O)_8C_{10}H_{21}$	2.8	2.5

[a] SE, after sonication (2−5 min); error ±0.1 nm. [b] Error ±0.2 nm. [c] SE;[15] error ±0.2 nm. [d] SPR.[15] [e] Ellipsometry;[28] error ±0.2 nm. [f] Ellipsometry;[23] error ±0.05 nm.

1 and **3** comparable to those obtained for the SAMs of their *n*-alkanethiol counterparts.[17]

RAIRS data showed that the THEO segments of **1**−**4** adopt a 7/2 helical structure oriented normal to the substrate which corresponds to the folded-chain crystal (FCC) polymorphic form of crystalline poly(ethylene oxide) (PEO).[18] Although PEO may hydrate to approximately 1 water molecule/EO unit,[19] neutron reflectivity data showed that little or no hydration of the THEO segment of $HS(EO)_6C_{18}H_{37}$ (**3**) accompanied the incorporation of mellitin into a HBM composed of **3** and partially deuterated dimyristoylphosphatidylcholine (DMPC-d_{54}).[20] These data suggest that the highly ordered SAMs of **1**−**4** may not easily hydrate or provide sufficient space for protein incorporation.

Previous reports suggest that the length of oligo(ethylene oxide) (OEO) segments can be important in determining SAM configuration or function. For example, Prime and Whitesides[21] studied nonspecific protein adsorption on SAMs of $HS(CH_2)_{11}O(EO)_xH$, where $x = 1-7$. Protein adsorption was found to be inhibited when $x \geq 3$. In this series, significant structural information for the OEO segment has only been reported for **5**, $x = 6$ (see Table 1).[22] In another study involving monolayer films on water and Au, Lang et al.[14] showed that the length of the EO segment influenced the SAM structure of the thiolipids {$[S(EO)_xR]_2$, where R = dialkylglycerophosphatidyl and $x = 1-3$}. Most recently, Valiokas et al.[23] discussed OEO structural characteristics for the SAMs of $HS(CH_2)_{15}CONH(EO)_xH$, where $x = 1$, 2, 4, and 6, and concluded a helical structure for $x = 6$, **6** (see Table 1).[24]

In this paper, we compare the structures for the SAMs of the series $HS(EO)_xR$ on Au, where $x = 4-8$ and R = $C_{10}H_{21}$. Our interest in this homologous series of increasing EO length is based on two very different ideas. On the one hand, if the 7/2 helix is not present with shorter or longer 1-thiaoligo(ethylene oxide) (TOEO) segments, the SAMs would most likely be less ordered relative to **1** [$(EO)_6$]. In this case, we would have more interesting SAMs, particularly the longer EO analogues, to provide a disordered polar region near the Au for HBM constructs. On the other hand, if the TOEO structural characteristics of **1** (a 7/2 helix oriented normal to the substrate[25]) are present in other members of the series, then the film thickness would increase in a predictable manner with an increase in the number of EO units.[26] In this case, these SAMs could provide the basis of an organic thin-film thickness standard in which the film structure would be independent of the film thickness. This is important because, for many measurements, changes in the film structure are difficult to distinguish from changes in the film thickness. This type of standard would be useful in a variety of measurements such as ellipsometry, electrochemistry, neutron and X-ray reflectivity, surface plasmon resonance (SPR), X-ray photoelectron spectroscopy, secondary ion mass spectroscopy, and other film measurement techniques.

Materials and Methods[27]

Hexa(ethylene oxide), 1-bromodecane, thioacetic acid, poly(ethylene glycol) (average molecular weight = 300), and hexamethylphosphoramide (HMPA) were purchased from Aldrich Chemical Co. (Milwaukee, WI). Tetrahydrofuran (THF; Mallinckrodt AR, North Strong Scientific, Phillipsburg, NJ) and HMPA were distilled from calcium hydride. THF was distilled under nitrogen immediately before use, whereas HMPA was distilled and stored under nitrogen over 0.3 nm molecular sieves. All other solvents (AR grade) were used without purification.

Synthesis. Compounds **7** [$(EO)_4$], **8** [$(EO)_5$], **9** [$(EO)_7$], and **10** [$(EO)_8$] were prepared in a fashion similar to that of **1**−**4** [$(EO)_6$].[15] The alkylation of PEO (average molecular weight = 300), using 1-bromodecane was carried out according to published procedures.[28] The crude mixture of alkylated PEO was converted to a mixture of the monobromo compounds, $Br(EO)_xR$, where R = $C_{10}H_{21}$ and pure bromo precursors for [$(EO)_4$]−[$(EO)_8$] were subsequently obtained by repeated flash chromatography (silica gel) [R_fs for $(EO)_4$, $(EO)_5$, and $(EO)_6$ = 0.67, 0.49, and 0.31, respectively (50% ethyl acetate/hexane), and those for $(EO)_7$ and $(EO)_8$ = 0.56 and 0.41, respectively (100% ethyl acetate)]. Mass spectroscopic data indicated that each bromo precursor was free of higher and lower EO homologues. The purified bromo precursors were converted to the thiols as described previously.[15,28] Structural assignments were made from proton nuclear magnetic resonance (^{1}H NMR) and high-resolution mass spectrom-

(17) Glazier, S.; Vanderah, D. J.; Plant, A. L. Manuscript in preparation.

(18) Kobayashi, M.; Sakashita, M. *J. Chem. Phys.* **1992**, *96*, 748. In FCC−PEO, the EO units are aligned such that the corresponding oxygens from molecule to molecule are colocated in planes parallel to the substrate surface, whereas in ECC−PEO, the corresponding oxygen atoms from molecule to molecule are not aligned.

(19) Lüsse, S.; Arnold, K. *Macromolecules* **1996**, *29*, 4251.

(20) Kreuger, S.; Meuse, C. W.; Majrzak, C. F.; Plant, A. L. Manuscript in preparation.

(21) Prime, K. L.; Whitesides, G. M. *J. Am. Chem. Soc.* **1993**, *115*, 10714.

(22) Harder, P.; Grunze, M.; Dahint, R.; Whitesides, G. M.; Laibinis, P. E. *J. Phys. Chem.* **1998**, *102*, 426. The spectra of **5** were found to be variable, ranging from "crystalline" to amorphous. A predominantly helical structure oriented normal to the substrate was concluded for "crystalline-like" **5** based largely on RAIRS data. The dominant feature in the 800−1500 cm^{-1} region for "crystalline-like" **5** is broad absorption bands from 1114 to 1145 cm^{-1}. These absorption bands do not correlate with either FCC− or ECC−PEO.[18]

(23) Valiokas, R.; Svedhem, S.; Svensson, S. C. T.; Liedberg, B. *Langmuir* **1999**, *15*, 3390.

(24) For **6**, a helical structure similar to "crystalline-like" **5**[22] is proposed. The spectra of "crystalline-like" **5** and **6** are remarkably similar in the 800−1500 cm^{-1} region, suggesting either disordered conformations or a mixture of helical structures.

(25) For the Au (1 1 1) surface, the SAM of **1** is nearly perfectly commensurate with the substrate lattice. The cross-sectional area of the THEO segment of **1** (21.38 Å^2) nearly perfectly matches the idealized packing density (21.4 Å^2/thiolate) of a $(\sqrt{3} \times \sqrt{3})R30°$ adlayer on (1 1 1) Au with S···S ≅ 0.5 nm.

(26) Takahashi, Y.; Tadokoro, H. *Macromolecules* **1973**, *23*, 672.

(27) The specifications of commercial products are for clarity only and do not constitute endorsement by NIST.

(28) Pale-Grosdemange, C.; Simon, E. S.; Prime, K. L.; Whitesides, G. M. *J. Am. Chem. Soc.* **1991**, *113*, 12.

etry (HRMS) data.[29] Sample purity (>98%) was determined from thin-layer chromatographic (TLC) analysis (one spot by TLC) and mass spectroscopic data (absence of parent ions for higher and lower EO homologues).

Gold substrates were prepared on silicon (1 0 0) wafers (Virginia Semiconductor, Fredricksburg, VA) previously coated with a layer of chromium by magnetron sputtering (Edwards Auto 306, U.K.) at a base pressure of $\sim 1 \times 10^{-7}$ mbar to a nominal thickness of 200 nm as described previously.[15] The monolayers were prepared by immersing the gold substrates in $\sim 1 \times 10^{-3}$ mol/L (mM) thiol solutions in 200 proof ethanol (Warner Graham Co., Cockeysville, MD) for a minimum of 3 days. Prior to all infrared spectroscopic ellipsometry (IRSE) and visible spectroscopic ellipsometry (SE) measurements, samples were removed from the thiol solution, sonicated for 2−5 min in ethanol, rinsed with ethanol, and then dried in a stream of dry nitrogen.

IRSE. IRSE measurements were performed as described elsewhere[30] on a Bruker Equinox 55 spectrometer (Billerica, MA) using 4 cm^{-1} resolution with two levels of zero filling. The measurements utilized a germanium double-diamond polarizer from Harrick Scientific Corp. (Ossining, NY) that was oriented at ~45° to the plane of incidence of the light and at ~45° to the gold surface. The VeeMax reflection optics, analyzer, analyzer rotation accessory, and control program were from Pike Instrument Co. (Madison, WI). The VeeMax was set and aligned to provide a 70° angle of incidence. The entire setup was sealed into the sample compartment using plastic so that only the 18 mm sampling hole of the VeeMax was open to the atmosphere. Data collection was automated using the Opus Macro language of the Bruker Equinox. Data analysis was performed using MathCad 7.0 (MathSoft Inc., Cambridge, MA) to calculate the ellipsometric properties Ψ, Δ, and D, the complex optical density function,[31] as described elsewhere.[30]

SE. Multiple-wavelength ellipsometric measurements were performed on a J. A. Woollam Co., Inc. (Lincoln, NE) M-44 spectroscopic ellipsometer aligned at an incidence angle 70.39° from the surface normal. Four measurements were obtained for each sample and, to reduce noise, 300 revolutions of the analyzer were accumulated. Thicknesses were calculated relative to the thickness of the SAM of [(EO)$_6$] on Au. Using a two-layer model, the optical constants of the Au layer were determined using a refractive index of 1.45 and a thickness of 3.1 nm for the SAM of [(EO)$_6$]. The optical constants for the Au were then used to determine the thicknesses of the SAMs, assuming a refractive index of 1.45 for all compounds. Modeling and thickness calculations were carried out using the WVASE software from J. A. Woollam Co.

SPR. The SPR device and the calibration of the SPR shift with respect to the optical thickness change were described previously.[32] Data collection was initiated with a flow of anhydrous ethanol over the bare gold surface (flow rate = 64 μL/s). Flow was then switched to an alkanethiol solution (~1 mM in ethanol). Data were taken at 2 s intervals throughout each experiment. Film thickness calculations were carried out assuming a refractive index of 1.45 for the organic film.

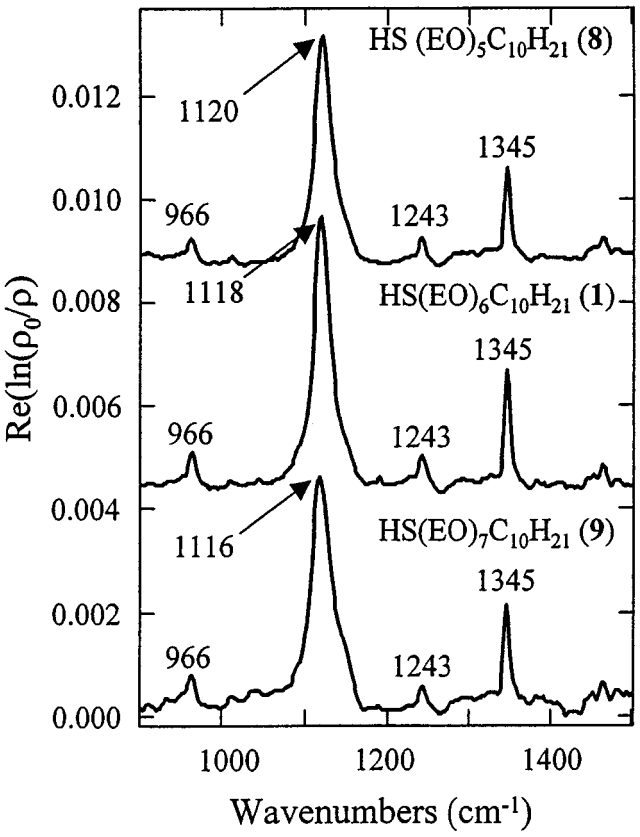

Figure 1. IRSE spectra of SAMs of [(EO)$_5$] [HS(EO)$_5$C$_{10}$H$_{21}$] {top}, [(EO)$_6$] [HS(EO)$_6$C$_{10}$H$_{21}$] {middle}, and [(EO)$_7$] [HS(EO)$_7$C$_{10}$H$_{21}$] {bottom} from 800 to 1500 cm^{-1}. Spectra offset for clarity.

Results and Discussion

IRSE spectra of the real (Re) part of the complex optical density function, D, for [(EO)$_5$], [(EO)$_6$], and [(EO)$_7$] in the 800−1500 cm^{-1} region are shown in Figure 1. The band positions for [(EO)$_6$] are essentially identical with the absorption bands in the RAIRS spectrum reported earlier,[15] indicating the FCC−PEO structure[18] for the TOEO segment. Figure 1 shows that the spectra of [(EO)$_5$] and [(EO)$_7$] are very similar to that of [(EO)$_6$]. Peaks near 966, 1118, 1243, and 1345 cm^{-1} indicate the presence of the FCC−PEO structure in all three TOEO segments.

Although the data in Figure 1 suggest that the structures of [(EO)$_5$], [(EO)$_6$], and [(EO)$_7$] are similar, close inspection reveals that [(EO)$_5$] and [(EO)$_7$] are slightly different from [(EO)$_6$]. The bands for [(EO)$_6$] are more intense than those for [(EO)$_5$] and [(EO)$_7$], in this region. In addition, a small but discernible higher frequency shoulder is observed on the 1116 cm^{-1} absorption band in the spectrum of [(EO)$_7$]. These both suggest that the TOEO segments of SAMs of [(EO)$_5$] and [(EO)$_7$] may consist of conformations other than FCC−PEO or may contain minor perturbations in the 7/2 helix, relative to [(EO)$_6$].

(29) HRMS data. **7**: HR FAB [M + 1]$^+$ calcd for $C_{18}H_{39}O_4S$ 351.25690; found 351.25767. **8**: HR CI [M + 1]$^+$ calcd for $C_{20}H_{43}O_5S$ 395.28311; found 395.28251. **9**: HR FAB [M + 1]$^+$ calcd for $C_{24}H_{51}O_7S$ 483.33554; found 483.33613. **10**: HR FAB [M + 1]$^+$ calcd for $C_{26}H_{55}O_8S$ 527.36176; found 527.36096.

(30) Meuse, C. W. Manuscript submitted for publication in *Langmuir*.

(31) $D = \ln(\rho_0/\rho)$, where $\rho = \tan(\psi)e^{i\Delta}$ and $\rho_0 = \tan(\psi_0)e^{i\Delta_0}$, and Ψ, Δ and Ψ_0, Δ_0 refer to the relative intensity of (Ψ) and the phase difference between (Δ) the parallel and perpendicular components of the polarized electric field vector interacting with the sample and reference, respectively. In IRSE data, Re[ln(ρ_0/ρ)] is equivalent to Re[ln($R_{p_o}/R_{s_o}/R_p/R_s$)], where Re is the real part of the complex number, R_v refers to the reflection coefficients of the light polarized || or p and ⊥ or s to the plane of incidence, and the subscript 0 refers to reference measurements acquired without the SAM present. ln($R_{p_o}/R_{s_o}/R_p/R_s$) can be converted to RAIRS data, log(R_{p_o}/R_p), by converting between ln and log because the s components of the reflection coefficients are ~0 for a high angle of incidence on a metal surface.

(32) Silin, V.; Weetall, H.; Vanderah, D. J. *J. Colloid Interface Sci.* **1997**, *185*, 94.

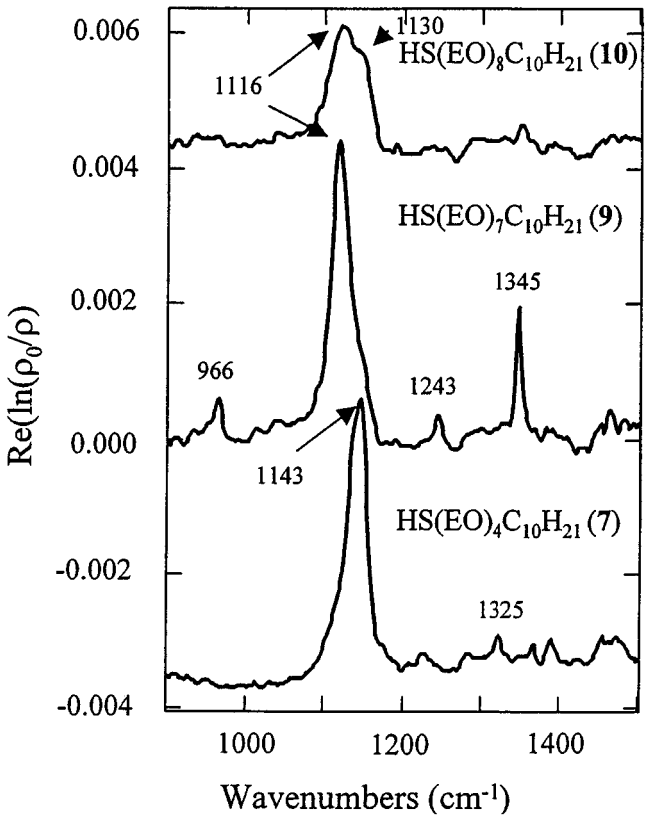

Figure 2. IRSE spectra of SAMs of $[(EO)_8]$ $[HS(EO)_8C_{10}H_{21}]$ {top}, $[(EO)_7]$ $[HS(EO)_7C_{10}H_{21}]$ {middle}, and $[(EO)_4]$ $[HS(EO)_4C_{10}H_{21}]$ {bottom} from 800 to 1500 cm^{-1}. Spectra offset for clarity.

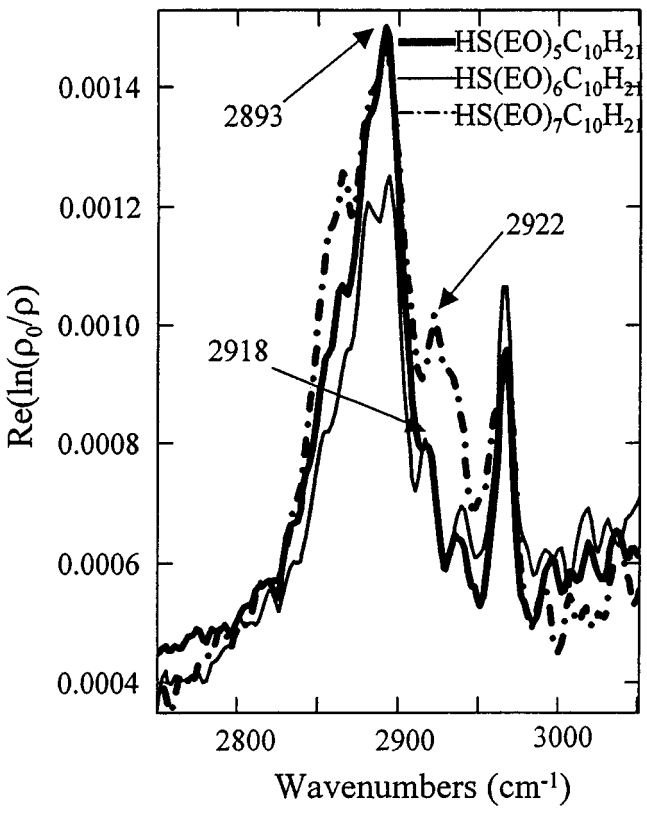

Figure 3. IRSE spectra of SAMs of $[(EO)_5]$ $[HS(EO)_5C_{10}H_{21}]$ {■}, $[(EO)_7]$ $[HS(EO)_7C_{10}H_{21}]$ {– · – }, and $[(EO)_6]$ $[HS(EO)_6C_{10}H_{21}]$ {—} from 2700 to 3100 cm^{-1}.

Another difference is the position of the most intense band [$A_2(6)$[18]]. This band appears at 1118 cm^{-1} in the spectrum of $[(EO)_6]$ but appears at 1120 and 1116 cm^{-1} in the spectra of $[(EO)_5]$ and $[(EO)_7]$, respectively. The most likely explanation for this bathochromic shift trend of ~2 cm^{-1}/additional EO unit is that the TOEO segments of $[(EO)_5]$ and $[(EO)_7]$ may not correlate exactly with the PEO segments. The spectral analysis of the FCC and extended-chain crystal (ECC) polymorphic forms of PEO[18] assumes an infinitely long, structurally homogeneous polymeric chain. In this series the TOEO segments are relatively short, differ in length, and have different functional groups at the termini—a Au–S bond on one end and a hydrocarbon chain on the other end. These differences might be expected to alter the band position slightly.

The IRSE spectra of $[(EO)_4]$, $[(EO)_7]$, and $[(EO)_8]$ in the 800–1500 cm^{-1} region are shown in Figure 2. The bands at 1345, 1243, 1116, and 966 cm^{-1} for $[(EO)_7]$ are not observed in the spectrum of $[(EO)_4]$. The 1143 cm^{-1} absorption band for $[(EO)_4]$, assigned as a C–O–C stretching vibration, suggests a dramatic conformational change from the FCC–PEO structures of $[(EO)_5]$, $[(EO)_6]$, and $[(EO)_7]$ and is similar to that obtained for the SAM of $HS(CH_2)_{11}(OCH_2CH_2)_3OCH_3$ (**11**) on Ag (1145 cm^{-1}),[22] with some increase in asymmetry. The presence of an absorption band at 1325 cm^{-1} and the absence of an absorption band at 1352 cm^{-1}, previously assigned to the wagging mode of the glycol C–C trans and C–C gauche conformations, respectively,[22] are evidence that the TOEO segment of $[(EO)_4]$ exists in a predominantly trans conformation, as was concluded for **11** on Ag. The spectrum of $[(EO)_4]$ does not show the 1313 cm^{-1} band of **11** on Ag, tentatively assigned as a coupled CH_2 wagging mode.[22] The 1313 cm^{-1} band may be absent or attenuated in $[(EO)_4]$ as result of a different orientation in the transition moment due a different cant angle, which is typically larger for SAMs on Au (~30°) than for SAMs on Ag (7–14°). Alternatively, the attenuation or absence of the 1313 cm^{-1} band may also be due to the different packing densities of SAMs on Ag and Au. The more densely packed trans-extended SAM of **11** on Ag[22] may be more conducive to coupling of the CH_2 wagging modes than the less densely packed trans-extended SAM of $[(EO)_4]$ on Au.

In the spectrum of $[(EO)_8]$ the most prominent absorption band appears at 1116 cm^{-1}, similar to the spectrum of $[(EO)_7]$, and could be assigned as the $A_2(6)$ band of the FCC–PEO structure. However, Figure 2 shows the attenuation or absence of other absorption bands characteristic of the FCC–PEO structure—1345, 1243, and 966 cm^{-1} for $A_2(4)$, $A_2(5)$, and $A_2(7)$, respectively. Absorption bands at ~1130 cm^{-1} [the higher wavenumber shoulder on the $A_2(6)$ band] and 1350 cm^{-1} are assigned to the C–O–C stretching vibration and the CH_2 gauche wagging mode, respectively. These bands are also present in the infrared spectra of PEO at 100 °C[33] and to "amorphous" SAMs of **5**[22] and are indicative of disorder. This dichotomy indicates a mixture of conformations. We conclude that while the SAM of $[(EO)_8]$ contains some of the helical FCC–PEO conformation, it is generally disordered. Thus, extension of the TOEO segment by only 2 EO units results in a significant change from the structure of $[(EO)_6]$.

The IRSE spectra of $[(EO)_5]$, $[(EO)_6]$, and $[(EO)_7]$ in the 2700–3100 cm^{-1} region are shown in Figure 3. This region is complicated by overlap of the C–H stretching contributions from both the TOEO and the alkyl segments.

(33) Dissanayake, M. A. K. L.; Frech, R. *Macromolecules* **1995**, *28*, 5312.

Analysis of this spectral region supports the TOEO structural assignments and provides evidence on the order of some of the $C_{10}H_{21}$ segments but does not allow a determination of the alkyl chain orientations. The presence of the FCC−PEO structure, for each of these compounds, is indicated by the prominent absorption band at 2893 ± 1 cm^{-1}, assigned to the CH_2 symmetric stretch of crystalline PEO.[22,34] In addition, the spectra from 2910 to 2950 cm^{-1} are informative. The d$^-$,ν_a(CH_2) band appears at 2918 cm^{-1} for [(EO)$_5$] and [(EO)$_6$] and 2922 cm^{-1} for [(EO)$_7$]. The position of this band at 2922 cm^{-1} for [(EO)$_7$] is similar to that for the SAM of *n*-decanethiol[11] and *n*-undecanethiol,[35] suggesting comparable order for the $C_{10}H_{21}$ segment. Higher order for the alkyl segments in [(EO)$_5$] and [(EO)$_6$] as suggested by the position of the d$^-$,ν_a(CH_2) band at 2918 cm^{-1} is possible but not likely. The position of this band in [(EO)$_5$] and [(EO)$_6$] may be shifted to this lower frequency because of overlap with the more intense TOEO C−H bands. In contrast, the altered TOEO of [(EO)$_4$] and [(EO)$_8$] produced very different C−H stretching signatures (data not shown) compared to [(EO)$_5$], [(EO)$_6$], and [(EO)$_7$] (Figure 3). These new patterns of TOEO and alkyl bands, as will be reported subsequently, are difficult to interpret compared to [(EO)$_5$], [(EO)$_6$], and [(EO)$_7$], whose structures can be inferred by correlation to analogous deuterated compounds.

Analysis of the C−H stretching region revealed another interesting observation. The spectra of the series ([(EO)$_4$], [(EO)$_5$], [(EO)$_6$], [(EO)$_7$], [(EO)$_8$]) varied with time over a period of several days. We attribute this to slow ordering of the SAMs, as has been suggested in the SAMs of other amphiphiles.[14] The details of these changes will be reported in a separate paper.[36]

IRSE spectra of the imaginary part of the complex optical density function (data not shown) can be used to determine the thicknesses of monolayer films.[30] The preliminary analysis of our data indicated film thicknesses on the order of 3.0 nm for all samples. The film thicknesses increased in the order [(EO)$_8$] < [(EO)$_5$] < [(EO)$_6$] < [(EO)$_7$] < [(EO)$_4$]. This is far from the order we expected. Simply on the basis of the increasing number of EO units, and thus the increasing number of atoms in the chains, we would expect film thicknesses to increase in the order [(EO)$_4$] < [(EO)$_5$] < [(EO)$_6$] < [(EO)$_7$] < [(EO)$_8$]. To be certain of our results, we decided to utilize methods based in the visible region of the spectrum where the films do not absorb and complicate the determination of the optical constants.

The adsorption and desorption of [(EO)$_4$], [(EO)$_5$], [(EO)$_6$], [(EO)$_7$], and [(EO)$_8$] were studied with SPR under continuous-flow conditions similar to those reported earlier.[15] Thicknesses for [(EO)$_4$], [(EO)$_5$], [(EO)$_6$], [(EO)$_7$], and [(EO)$_8$] as a function of time are shown in Figure 4. These data show that the kinetics of formation in this homologous series are similar but that the desorption kinetics upon the initiation of ethanol washing are different in that only [(EO)$_4$] and [(EO)$_5$] show significant desorption. Using models discussed previously,[15] desorption kinetic constants of 7.1 ± 0.5 × 10^{-5}/s and 9.8 ± 0.5 × 10^{-4}/s were found for [(EO)$_4$] and [(EO)$_5$], respectively, compared to 1.1 ± 0.5 × 10^{-4}/s previously reported for **4** [HS(EO)$_6$C$_{18}$H$_{37}$].[15] These data suggest physisorbed material as found earlier for related compounds.

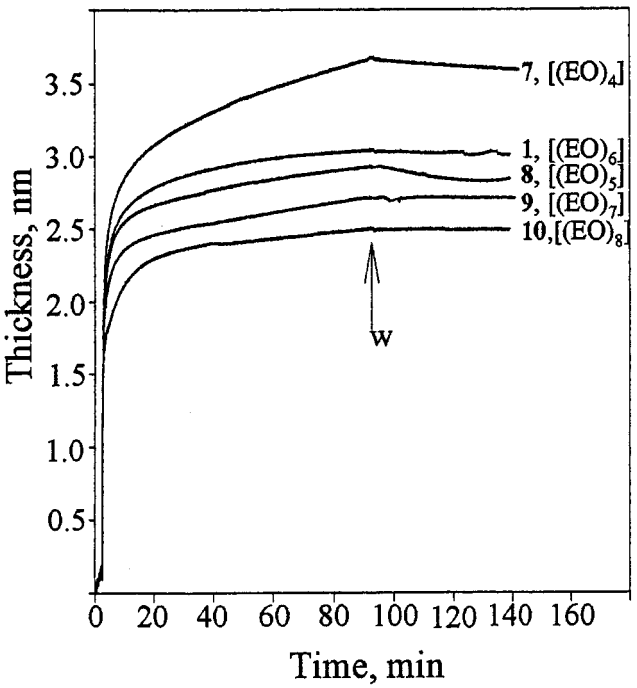

Figure 4. SPR surface thickness measurements of [(EO)$_4$], [(EO)$_5$], [(EO)$_6$], [(EO)$_7$], and [(EO)$_8$] under continuous conditions as a function of time at 22 °C. The thickness was calculated from the position of the SPR minimum and an assumed refractive index of 1.45 for the SAM. w = washing with anhydrous ethanol.

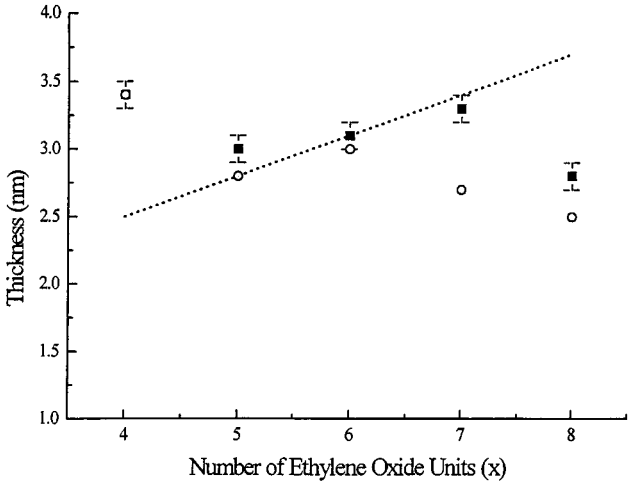

Figure 5. Plot of SE (■) and SPR (○) thicknesses of the SAMs of [(EO)$_4$], [(EO)$_5$], [(EO)$_6$], [(EO)$_7$], and [(EO)$_8$]. The dashed line is the SAM thickness increase expected[26] if the series were isostructural with the TOEO segments in the FCC−PEO conformation.

Film thicknesses for [(EO)$_4$], [(EO)$_5$], [(EO)$_6$], [(EO)$_7$], and [(EO)$_8$], as calculated from the SPR data (t = 140 min, after ethanol washing; Figure 4), and for [(EO)$_6$]−[(EO)$_8$], as calculated from ellipsometric and SE data, are given in Table 1. Similar to the IRSE measurements, the SPR data indicated [(EO)$_4$] to be the thickest monolayer (3.4 nm) and [(EO)$_8$] to be the thinnest monolayer (2.5 nm), suggesting different structures and/or packing densities. Figure 5 is a plot of the SPR and SE thicknesses for [(EO)$_4$], [(EO)$_5$], [(EO)$_6$], [(EO)$_7$], and [(EO)$_8$] as a function of increasing EO length. The dashed line in Figure 5 indicates the expected thicknesses for the SAMs if the series is isostructural with [(EO)$_6$], on the basis of the unit cell dimensions of the 7/2 helical structure of crystalline PEO

(34) Miyazawa, T.; Fukushima, K.; Ideguchi, Y. *J. Chem. Phys.* **1962**, *37*, 2764.

(35) Walczak, M. M.; Chung, C.; Stole, S. M.; Widrig, C. A.; Porter, M. D. *J. Am. Chem. Soc.* **1991**, *113*, 2370.

(36) Figures 1−3 show the SAM IRSE data after 3 days in 1 mM thiol solutions.

(∼0.28 nm/EO).[26] The near-identical thicknesses observed for $[(EO)_5]$, $[(EO)_6]$, and $[(EO)_7]$ as well as the large deviations from the dashed line for $[(EO)_4]$ and $[(EO)_8]$ indicate structural or packing density variation over the entire range of x. Monolayer thicknesses for $[(EO)_4]$, $[(EO)_5]$, $[(EO)_6]$, $[(EO)_7]$, and $[(EO)_8]$ from SE are in good agreement with those from the SPR technique. The slight differences between the SE and the SPR results are ascribable to differences in the time of SAM formation (SPR, 140 min; SE, 3 days) and the fact that the SPR data are acquired in the presence of ethanol, as discussed previously.[15] As a result all subsequent discussion will use SE thickness values.

The calculated thickness of $[(EO)_4]$, 3.4 nm, exceeds the theoretical thickness for all possible structural models. The maximum thickness for $[(EO)_4]$ is ∼2.9 nm, assuming *both* an all-trans conformation over the entire molecule and orientation normal to the surface. As mention earlier, it is unlikely that $[(EO)_4]$ would have a small (<10°) cant angle. A more plausible structure is a predominantly all-trans conformation with a cant angle of ∼30°, similar to those of alkanethiols. For this structure of $[(EO)_4]$, a thickness of ∼2.5 nm is expected. The large difference, ∼0.9 nm, between the SE thickness and the thickness predicted by our model may be due to three factors. First, physisorbed molecules are present on or between chemisorbed molecules. SPR data (Figure 4) indicate thickness values that are greater than theoretical values obtained for $[(EO)_4]$ in <5 min, similar to that obtained for **3** $[HS(EO)_6C_{18}]$,[15] and a calculated final thickness of 3.3 nm at $t = \infty$. Noteworthy here, however, is the fact that, unlike **3**, the SE thickness of $[(EO)_4]$ exceeds the theoretical thickness after sonication (2−5 min). Second, the optical constants of the SAMs of $[(EO)_4]$ and $[(EO)_6]$ may be different. The indices of refraction, n, and/or the extinction coefficients, k, for **1** may be different from those for $[(EO)_4]$ because of differences in conformations or packing densities. In the SE calculations a change in n from 1.45 to 1.475 lowered the thickness of $[(EO)_4]$ from 3.3 to 3.1 nm. Third, the optical constants of the Au for the SAMs of $[(EO)_4]$ and $[(EO)_6]$ may be different due to differences in the Au sulfur interface. Collins et al.[37] discuss this interface as an approximately 0.2 nm layer containing unspecified optical constant components from both the Au and the sulfur atom. A 1% change in k for the Au can lower the thickness from 3.0 to 2.5 nm.

For $[(EO)_8]$, an ordered structure, like $[(EO)_6]$ or $[(EO)_4]$, would result in the thickest SAM (>3.7 nm) of the series. The large difference, >0.9 nm, between the calculated and the expected thicknesses is attributed to a mixture of ordered and disordered conformations, as deduced from the IRSE spectrum. SAMs containing disordered conformations are likely to be less well packed and have fewer molecules on the surface, resulting in smaller optical thicknesses than expected, as has been reported previously.[28] In addition, differences in the optical constants for the helical and amorphous conformations in $[(EO)_8]$ may also contribute to the thickness discrepancy.

For $[(EO)_5]$ the calculated thickness, 3.0 nm, is much closer to the dashed line in Figure 5 than thicknesses for $[(EO)_4]$ and $[(EO)_8]$ and is slightly thicker than expected, 2.8 nm. This, coupled with the IRSE data discussed earlier, indicates that the structure of $[(EO)_5]$ is more similar to $[(EO)_6]$ and thus would be expected to have similar optical constants. However, the small but significant deviation from the expected film thickness (0.2 nm) suggests that the structure of the SAM of $[(EO)_5]$ cannot be exactly the same as that of the SAM of $[(EO)_6]$. The SE data suggest that the TOEO segment of $[(EO)_5]$ is a mixture of the FCC−PEO conformation and other conformations, with the former predominating. We believe that the SAM of $[(EO)_5]$ may contain trans conformations due to the predominance of that conformation in the lower homologue $[(EO)_4]$, and because of the coexistence of the FCC−PEO, conformation plus trans conformations would result in a thicker SAM for $[(EO)_5]$ relative to a perfectly helical FCC−PEO structure.

For $[(EO)_7]$ the calculated thickness, 3.3 nm, is also close to that for $[(EO)_6]$ (dashed line in Figure 5) but is thinner than expected (0.1 nm) from the idealized FCC−PEO model. Earlier arguments suggested that $[(EO)_7]$ may not exist solely in the FCC−PEO conformation. Noteworthy here is the fact that the $A_2(6)$ band in the IRSE spectrum of $[(EO)_7]$, which has one more EO unit than $[(EO)_6]$, is less intense than the $A_2(6)$ band in the spectrum of $[(EO)_6]$. Also, the shoulder on the $A_2(6)$ band of $[(EO)_7]$ corresponds to the more prominent shoulder (∼1130 cm^{-1}) on the $A_2(6)$ band of $[(EO)_8]$. This suggests that a small percentage of the TOEO segments of $[(EO)_7]$ adopts disordered conformations similar to those of $[(EO)_8]$. The presence of disordered conformations coexisting with the FCC−PEO conformation in the SAM of $[(EO)_7]$ would be expected to decrease the film thickness.

The IRSE and SE data indicate that a near-perfect FCC−PEO structure is found only for $[(EO)_6]$ and that no subset of this series is isostructural with $[(EO)_6]$, as would be necessary for a thin film thickness standard. However, the differences from $x = 5-7$ are small. We are preparing an analogous series, with longer alkyl groups, which might form SAMs that are isostructural over some range of x.

Conclusions

IRSE, SE, and SPR data show that the structures of the SAMs of $HS(EO)_xC_{10}H_{21}$ on Au differ considerably over a relatively narrow range of x. Significant structural changes are observed by increasing the TOEO unit by 1 in two cases, $x = 4 \rightarrow 5$ and $x = 7 \rightarrow 8$, in this series. For $x = 4$, the molecules adopt a predominantly trans conformation similar to that reported for the SAM of $HS(CH_2)_{11}(OCH_2CH_2)_3OCH_3$ on Ag.[22] For $x = 5$ and 7, the TOEO segments adopt a 7/2 helical structure oriented normal to the substrate and the $C_{10}H_{21}$ adopts a predominantly trans conformation similar to that of $[(EO)_6]$, $x = 6$.[15] Minor structural differences for $x = 5$ and 7 are suggested, indicating that the series is not isostructural over the range of x and thus has no utility as a thickness standard. For $x = 8$, a significantly less ordered SAM similar in many respects to that observed in related compounds is obtained.[22] The loss of the highly ordered 7/2 helix for $HS(EO)_8C_{10}H_{21}$ is potentially valuable for HBM studies. SAMs of this compound may more closely "mimic" the supporting matrixes of natural bilayers and provide less hindrance for the incorporation of transmembrane and integral-membrane proteins.

LA9916833

(37) Collins, R. W.; Allara, D. L.; Kim, Y.-K.; Lu, Y.; Shi, J. In *Characterization of Organic Thin Films*; Ulman, A., Ed.; Butterworth-Heineman: Boston, 1995.